Available online at www.sciencedirect.com
SCIENCE DIRECT®
Journal of Power Sources 122 (2003) 169–173
JOURNAL OF POWER SOURCES
www.elsevier.com/locate/jpowsour

Thin-film lithium and lithium-ion batteries with electrochemically deposited molybdenum oxysulfide cathodes

V. Yufit [b], M. Nathan [b,*], D. Golodnitsky [a], E. Peled [a]

[a] *Faculty of Exact Sciences, School of Chemistry, Tel Aviv University, Tel Aviv 69978, Israel*
[b] *Department of Electrical Engineering and Physical Electronics, Tel Aviv University, Tel Aviv 69978, Israel*

Received 4 November 2002; received in revised form 9 February 2003; accepted 17 February 2003

Abstract

Thin-film molybdenum oxysulfide films were deposited electrochemically on both nickel foils and nickel-coated silicon substrates, and used as cathodes in lithium battery cells that included a lithium anode and a hybride gel electrolyte (HPE) or solid polymer electrolyte (SPE). X-ray diffraction (XRD) and X-ray photoelectron spectroscopy (XPS) characterizations indicated that the sub-micron thick MoO_yS_z films were amorphous, with the stoichiometry of the films varying with depth. A Li/HPE/MoO_yS_z on nickel and nickel-coated silicon ran at $i_d = i_{ch} = 100\,\mu A/cm^2$ and room temperature for 1000 charge/discharge cycles with 0.05% per cycle capacity loss and 100% Faradaic efficiency. Cells with SPE cycled at 125 °C showed a higher per cycle capacity loss of 0.5%.

Keywords: Lithium and lithium-ion thin-film batteries; MoS_2 thin-film cathode; Electrochemical cathode deposition

1. Introduction

Modern microelectronic and MEMS devices increasingly require miniaturized power sources or "microbatteries", of which those based on lithium or lithium-ion are the most attractive in terms of specific volumetric and gravimetric capacity. New thin-film materials for cathodes and low cost preparation methods of these films are key to making such microbatteries viable in performance/cost terms. At present, the main deposition techniques for making thin-film cathodes include chemical vapor deposition (CVD), sputtering, spray pyrolysis and evaporation, and, to a lesser degree, electrochemical methods. For example, Fragnaud et al. [1] prepared thin-film $LiCoO_2$ and $LiMn_2O_4$ cathodes in secondary lithium batteries using CVD and spray pyrolysis. Martin-Litas [2] and Levasseur [3] prepared tungsten oxysulfide (WO_yS_2) and molybdenum oxysulfide (MoO_xS_y) thin films, respectively by reactive radio-frequency (RF) magnetron sputtering. Polycrystalline tungsten disulfide thin films were electrodeposited on conducting glass plates in a galvanostatic route by Devadasan et al. [4], their use directed toward photo-electrochemical solar cells.

MoS_2 is a very attractive material for Li and Li-ion battery applications [5]. Miki et al. [6] synthesized a MoS_2 powder as the cathode active material for lithium secondary batteries using thermal decomposition of $(NH_4)_2MoS_4$ in a hydrogen gas flow at temperatures from 150 to 300 °C. They found that the MoS_2 thus formed was amorphous, and that the lithium diffusion coefficient into this amorphous material was higher by several orders of magnitude than that in the crystalline structure. Successful attempts to electro-deposit thin-film MoS_2 at room temperature were carried out by Ponomarev [7] and Patil [8]. In this work, we used the electrochemical method described by Ponomarev to deposit thin Mo sulfide cathodes, which were then tested in lithium battery cells during prolonged cycling. As shown below, various characterizations indicated that the deposited films were actually Mo oxysulfides.

2. Experimental

Thin film, nominally MoS_2 cathodes were prepared electrochemically in an aqueous 0.028 M solution of tetrathiomolibdate (MoS_4^{2-}) ions at a current density of $10\,mA/cm^2$. Deposition was carried out on both nickel foils and on nickel-coated silicon substrates, both pre-degreased in acetone and etched in concentrated nitric acid, with a graphite rod used as a counter electrode. The electroless

* Corresponding author. Tel.: +972-3-640-6909; fax: +972-3-642-2649.
E-mail addresses: nathan@eng.tau.ac.il (M. Nathan), golod@post.tau.ac.il (D. Golodnitsky).

0378-7753/03/$ – see front matter © 2003 Elsevier Science B.V. All rights reserved.
doi:10.1016/S0378-7753(03)00401-4

plating of pretreated silicon substrates was performed in a solution composed of $NiSO_4$, $Na_2H_2PO_2$ reducing agent, and sodium citrate as a complexing agent and buffer. In our experiments we used mainly solutions of freshly prepared tetrathiomolybdate formed in a chemical reaction in a solution of Na_2MoO_4 and Na_2S according to [7]. The pH of the solution was adjusted to 7–7.5 by addition of an appropriate amount of hydrochloric acid. The estimated mass of the cathode was about 0.24 mg/cm^2.

A JSM-6300 scanning microscope (Jeol Co.) equipped with a Link elemental analyzer and a silicon detector was used to study the surface morphology. X-ray diffraction (XRD) data were obtained with the use of a θ–θ Scintag powder diffractometer equipped with a Cu Kα source and a liquid-nitrogen germanium solid-state detector. X-ray photoelectron spectroscopy (XPS) tests of as-deposited films were performed with a monochromatic Al Kα source (1486.6 eV) in ultra-high vacuum (2.5×10^{-10} Torr) using a 5600 Multi-Technique System (Physical Electronics Inc., USA).

As-deposited samples of thin-film MoS_2 cathodes were dried in vacuum at about 100 °C. All subsequent handling of these materials took place under an argon atmosphere in a VAC glove box containing less than 10 ppm water. The electrochemical cells studied comprised a lithium anode, hybrid hybride gel electrolyte (HPE) or composite solid polymer electrolyte (SPE), and a MoS_2 cathode. For the Li-ion cells, electrochemically prepared lithiated graphite was used as an anode. The lithiation of graphite powder (expanded graphite produced by ITE Battery Research Institute) was carried out as given further. A polymer binder (polystyrene) was dissolved in toluene, and, after dissolution, expanded graphite powder (of a few μm average particle size) was added to the mixture. The resulting slurry was spread on a copper current collector using a doctor blade. This electrode was vacuum dried and assembled with lithium and an ion-conductive separator (Celgard soaked in 1 M $LiPF_6$ EC:DEC 1:1 (v/v)) in cells. After a few successive cycles, the cells were disassembled and each lithiated electrode was rinsed in DMC and vacuum-dried. The lithiated graphite electrode was then used as an anode in a Li-ion/HPE/MoS_2 on-silicon battery. The chosen polymer for HPE was a commercially available PVDF-2801 copolymer (Kynar). The PVDF powder was dissolved in high-purity cyclopentanone (Aldrich); fumed silica 130 (Degussa) and propylene carbonate (PC, Merck) were added, and the mixture was stirred at room temperature for about 24 h to get a homogeneous slurry. After complete dissolution, the slurry was cast on a Teflon support and spread with the use of a doctor blade. After complete evaporation of the cyclopentanone, a 13 mm diameter disc was cut from the polymer membrane. The disc was soaked in a 1 M $LiPF_6$ EC:DEC 1:1 electrolyte for 48 h. In order to ensure a complete exchange of the PC by the electrolyte, at least three fresh portions of electrolyte were used for each soaking. The solid composite polymer electrolyte $LiImide_1P(EO)_{20}EC_1$ 12% by volume (v/v) Al_2O_3 was prepared as described elsewhere [9]. All electrochemical tests were performed in hermetically sealed, 1 cm^2 electrode area, 2324 coin cells. Cell-cycling tests were carried out in a 16-bit Maccor 2000 Battery Tester at 10–100 μA/cm^2 over the voltage range of 2.4–1.3 V.

3. Result and discussion

According to Ponomarev et al. [7], the electrochemical reduction of the tetrathiomolybdate ion proceeds as follows:

$$MoS_4^{2-} + 2e + 2H_2O \rightarrow MoS_2 + 2SH^- + 2OH^- \quad (1)$$

During electrodeposition, smooth brown films are formed at the electrodes. In our depositions, similarly to [7] when the thickness of the deposits exceeded 1.5–2 μm, the layer

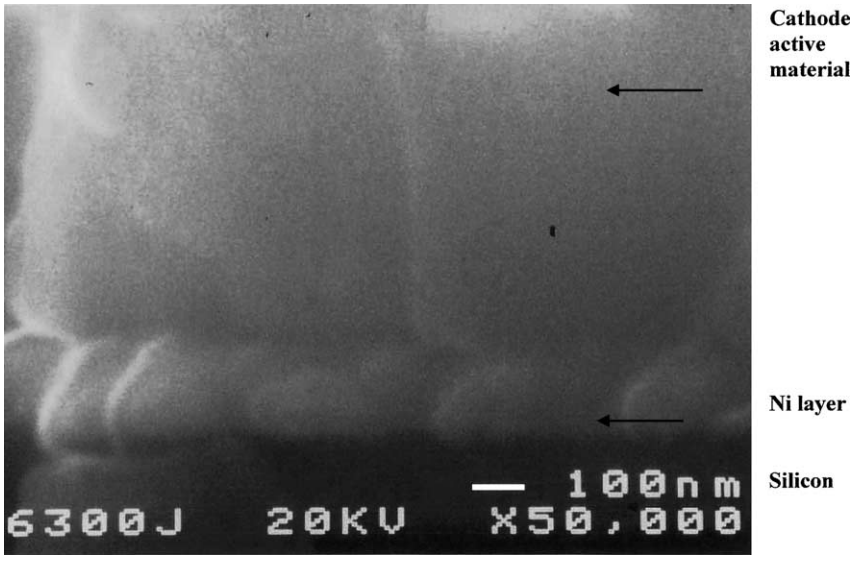

Fig. 1. SEM micrographs of the cross-section of a cathode deposited on nickel-coated silicon.

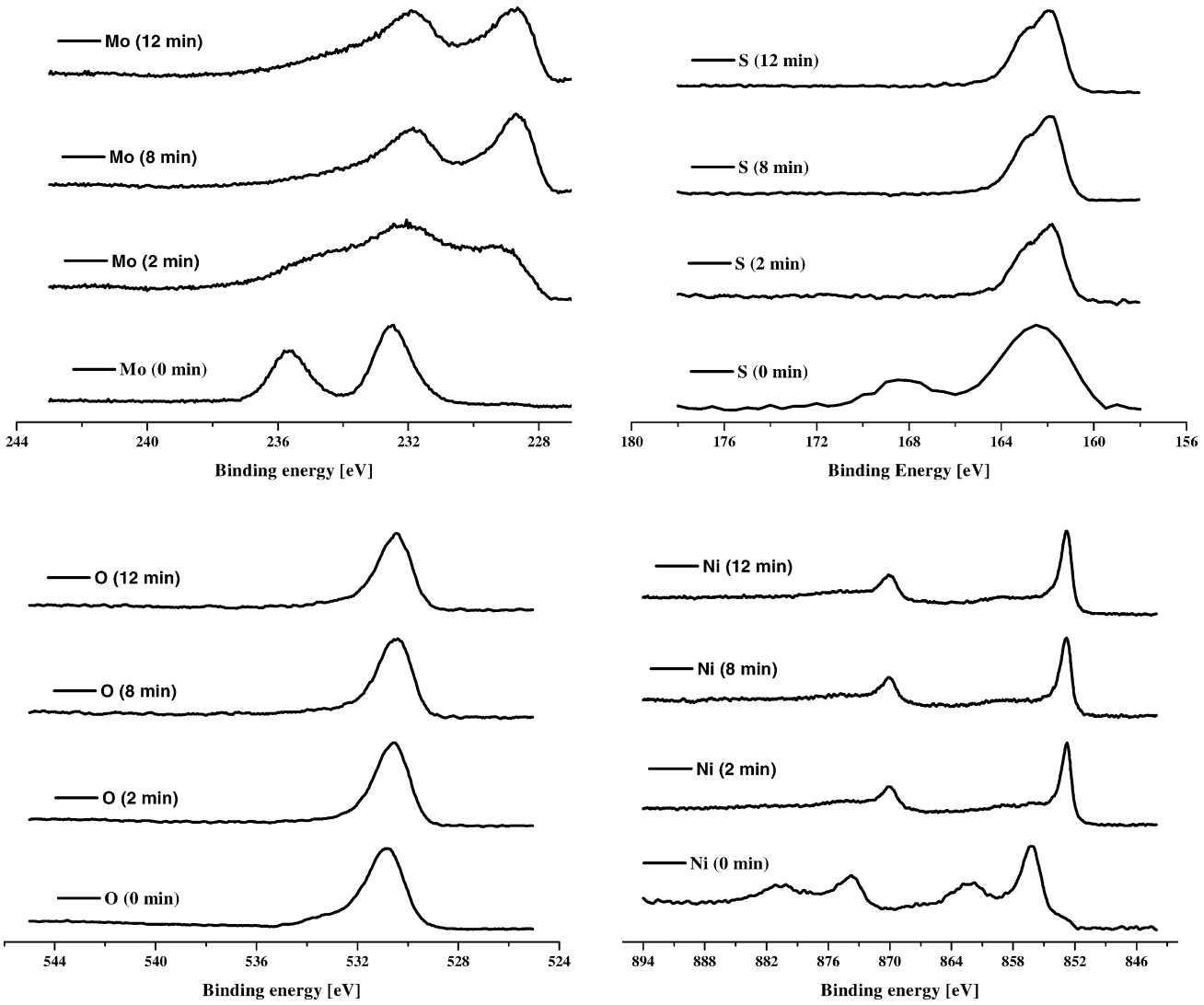

Fig. 2. shows the Mo 3d, S 2p, O 1s and Ni 2p XPS spectra of as-deposited films (0 min), as well as films after various depth profiling times.

started to peel off from the substrate. The optimal deposition time was therefore chosen to be 3–5 min.

Fig. 1 shows a SEM micrograph of the cross-section of a cathode deposited on nickel-coated silicon. The cathode layer is a compact, highly adherent film of about 300–600 nm thickness. A powder XRD analysis of such as-deposited films on nickel showed crystallographic peaks belonging to the nickel substrate alone. This may indicate that the electrodeposited film is mainly amorphous, in agreement with [7,10]. In order to get more precise information of the composition of the electrodeposited material, high-resolution XPS measurements were performed in the narrow window of 11.75 eV with a 0.05 eV per step. Fig. 2(a–d) shows Mo 3d, S 2p, O 1s and Ni 2p XPS spectra of as-deposited films before and after depth sputtering. A strong doublet at 232.5 and 235.7 eV is clearly seen in the molybdenum binding energy region. This doublet may be attributed to molybdenum oxide—MoO_3. A scarcely visible shoulder at 229.2 eV is related to a MoS_2 compound [11]. After 2 min of sputtering, the intensity of the 235.7 eV peak sharply decreases, the intensity of 229 eV peak increases, and the XPS bands overlap. These broad bands may indicate the presence of both Mo–S and Mo–O bonds. After 8 min of sputtering, the XPS peaks at 231.9 and 228.7 eV associated with molybdenum sulfide become dominating. The broad peaks with maximum at 162.5 and 168 eV in the S 2p XPS spectrum are characteristic of Mo–S and S–O bonds, respectively. The binding energy position of the S $2p_{3/2}$ peak can be attributed to a MoS_2 structure. Upon sputtering, the S–O peak vanishes and the molybdenum sulfide peak prevails. The typical Ni 2p doublet bands at 856.2 and 873.8 eV verify the presence of nickel oxides on the surface of the sample. A small shoulder at 852.8 eV, the intensity of which increases upon sputtering, is related to the metallic nickel substrate that underlies the molybdenum sulfide film. The broad O 1s peak at 530.8 eV can be attributed to molybdenum and nickel oxides. It seems likely that the composition of molybdenum oxides as function of the layer depth changes from

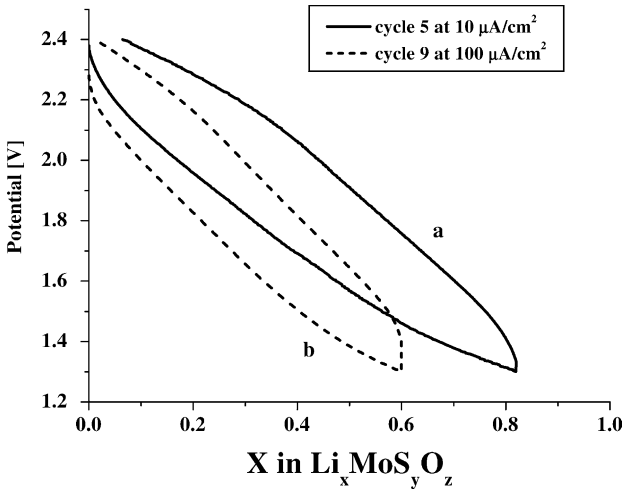

Fig. 3. Typical charge/discharge curves of a room temperature Li/HPE/MoO_yS_z cell with a cathode deposited on a nickel substrate. Cycling conditions: $V_{cut\text{-}off}$ = 1.3–2.4 V; $i_{dis} = i_{ch}$ = 10 μA/cm^2 (curve a); $i_{dis} = i_{ch}$ = 100 μA/cm^2 (curve b).

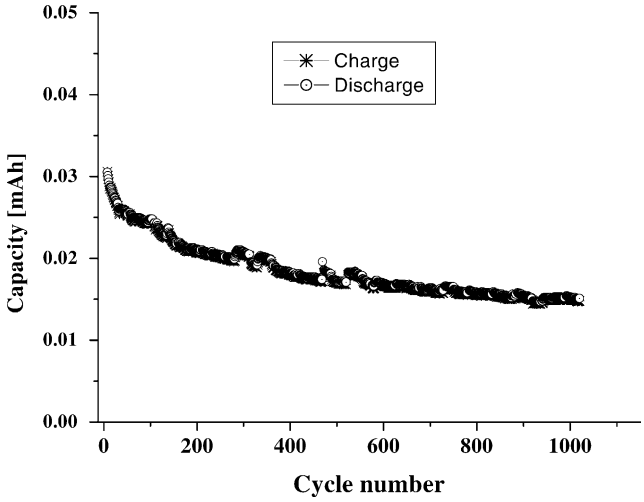

Fig. 4. Capacity vs. cycle number plots of the room temperature Li/HPE/MoO_yS_z cell with a cathode deposited on a nickel substrate. Cycling conditions: $V_{cut\text{-}off}$ = 1.3–2.4 V; $i_{dis} = i_{ch}$ = 100 μA/cm^2.

MoO_3 to MoO_2, possibly as a result of sputtering. The analysis of the elemental depth profile (not shown here) reveals the presence of large amounts of molybdenum oxide and a small concentration of molybdenum sulfide on the surface. In contrast, in the bulk of the electrodeposited compound, the concentration of MoS_2 is close to that of MoO_2. The electrochemical formation of amorphous molybdenum oxysulfide films, like MoO_yS_z obtained by RF sputtering [11,12] cannot be excluded as well. The determination of the precise stochiometry of the deposit is in progress. Incomplete covering of the substrate and/or possible porosity of the amorphous MoO_yS_z material may explain the appearance of NiO XPS peaks on the surface.

Fig. 3 shows typical charge/discharge curves of a Li/HPE/MoO_yS_z cell with the cathode deposited on a nickel substrate. The cell was cycled at room temperature with $i_d = i_{ch}$ = 10 μA/cm^2. The sloping character of the curves is typical of an insertion/de-insertion process into a single-phase host material according to the reaction (2).

$$MoO_yS_z + xLi^+ \rightarrow Li_xMoO_yS_z \quad (2)$$

We would like to emphasize that up to a 10-fold increase in the current density did not influence either the shape of the curves (Fig. 3b), or the degradation rate. The first cycle utilization of the cathode active material approached 85%. The Li/HPE/MoO_yS_z cell ran over 1000 successive cycles with 0.05% per cycle capacity loss and 100% Faradaic efficiency (Fig. 4).

Fig. 5 shows the plots of capacity loss and charging efficiency of a Li/HPE/MoO_yS_z cell with the cathode deposited on a nickel-coated silicon substrate. The cell was cycled at room temperature and at a 100 μA/cm^2 rate. As can be seen from Fig. 5, similar to the previous case, during more than 1000 reversible 100% depth of discharge (DOD) cycles, the degradation rate did not exceed 0.02% per cycle, and the Faradaic efficiency was close to 100%. Long-term cycling of the Li-ion/MoO_yS_z cells with a hybrid electrolyte exhibited 0.06% per cycle capacity loss under the same operating conditions.

Charge/discharge testing of a Li/LiImide$_1$P(EO)$_{20}$EC$_1$ 12% (v/v) Al_2O_3/MoO_yS_z cell was carried out at 125 °C (Fig. 6). While the same charge/discharge mechanism is expected in this electrochemical system, the degradation degree in Li/CPE/MoS_2 cell was higher: 0.5% per cycle. This may be caused by poor contacts and insufficient ionic mobility in the all-solid-state battery.

Finally, it is noteworthy that no self-discharge was detected in any of the Li/MoO_yS_z cells under investigation. Also, it was found that slow overdischarge to 0.2 V does not affect the subsequent cycling behavior of the Li/MoO_xS_y batteries.

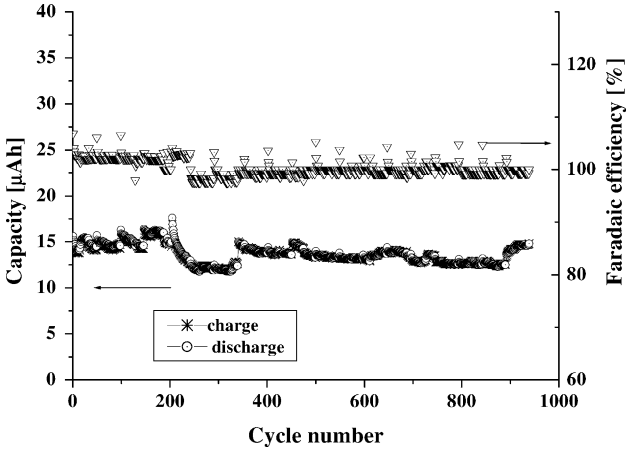

Fig. 5. Long-term cycling of the room temperature Li/HPE/MoO_yS_z cell with a cathode deposited on a nickel-coated silicon substrate. Cycling conditions: $V_{cut\text{-}off}$ = 1.3–2.4 V; $i_{dis} = i_{ch}$ = 100 μA/cm^2.

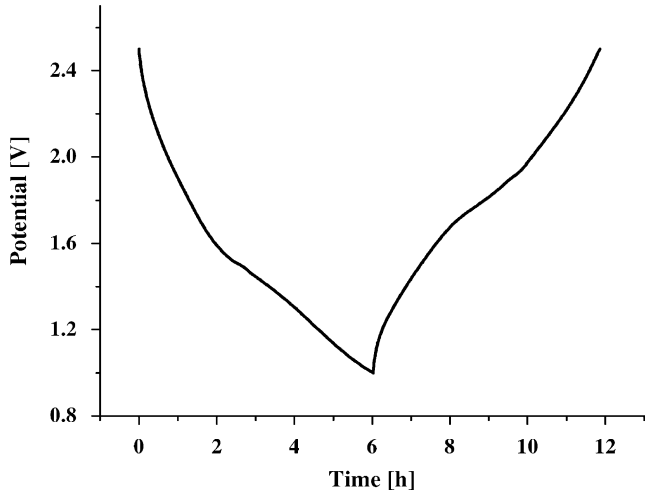

Fig. 6. Charge/discharge curves of a Li/LiImide$_1$P(EO)$_{20}$EC$_1$ 12% (v/v) Al_2O_3/MoO_yS_z cell. Cycling conditions: $V_{cut\text{-}off}$ = 1.0–2.45 V; $i_{dis} = i_{ch} = 10\,\mu A/cm^2$. $T = 125\,^{\circ}C$.

4. Conclusions

The nominally molybdenum sulfide films that were expected from Ponomarev's [7] electrochemical deposition process were found to include significant amounts of oxygen and be in fact molybdenum oxysulfides. They were successfully deposited on both nickel foils and nickel-coated silicon substrates and used as cathodes in lithium and lithium-ion batteries that included a lithium anode and either a HP or a SP electrolyte. The charge/discharge cycling of these cells indicated excellent room and high temperature behavior. A Li/HPE/MoO_yS_z-on-nickel cell ran at $i_d = i_{ch} = 100\,\mu A/cm^2$ and room temperature for 1000 charge/discharge cycles with 0.05% per cycle capacity loss and 100% Faradaic efficiency. The cell with the cathode deposited on nickel-coated silicon showed similar capacity loss and efficiency under the same operating conditions. Cells with SPE and cycled at 125 °C showed a higher per cycle capacity loss of 0.5%. In conclusion, we find that sub-micron thick, electrochemically deposited molybdenum oxysulfides, which are advantageous in their simple and inexpensive preparation method and in the fact that they are conformal to the shape of a substrate, can serve as excellent cathodes in thin-film Li and Li-ion cells.

Acknowledgements

We thank to Dr. L. Burstein and Dr. Yu. Rozenberg from the Wolfson Applied Materials Research Center for the conducting of the XPS and XRD measurements. We express our gratitude to Ms. E. Sverdlov from the Department of Electrical Engineering for the electroless coating of silicon samples.

References

[1] P. Fragnaud, R. Nagarajan, D.M. Schleich, D. Vujic, J. Power Sources 54 (1995) 362.
[2] I. Martin-Litas, P. Vinatier, A. Levasseur, J.C. Dupin, D. Gonbeau, J. Power Sources 97–98 (2001) 545.
[3] A. Levasseur, E. Schmidt, G. Meunier, D. Gonbeau, L. Benoist, G. Pfister-Guillouzo, J. Power Sources 54 (1995) 352.
[4] J.J. Devadasan, C. Sanjeeviraja, M. Jayachandran, J. Cryst. Growth 226 (2001) 67.
[5] R.R. Haering, J.A.R. Stiles, K. Brandt, US Patent Number 4224390 (1980).
[6] Y. Miki, D. Nakazato, H. Ikuta, T. Uchida, M. Wakihara, J. Power Sources 54 (1995) 508.
[7] E.A. Ponomarev, M. Neumann-Spallart, G. Hodes, C. Levy-Clement, Thin Solid Films 280 (1996) 86.
[8] R.S. Patil, Thin Solid Films 340 (1999) 11.
[9] D. Golodnitsky, G. Ardel, E. Strauss, E. Peled, Y. Lareah, Yu. Rosenberg, J. Electrochem. Soc. 144 (1997) 3484.
[10] A. Albu-Yaron, C. Levy-Clement, A. Katty, S. Bastide, R. Tenne, Thin Solid Films 361–362 (2000) 223.
[11] M.A. Baker, R. Gilmore, C. Lenardi, W. Gissler, Appl. Surf. Sci. 150 (1999) 255.
[12] L. Benoist, D. Gonbeau, G. Pfister-Guillouzo, E. Schmidt, G. Meunier, A. Levasseur, Solid State Ionics 76 (1995) 81.